社団法人 情報処理学会　研究報告
IPSJ SIG Technical Report

2004－CVIM－146　(1)
2004／11／11

オプティカルフローによる環境地図の取得と軌道制御

大西 直哉 †　井宮 淳 ††

† 千葉大学　自然科学研究科
†† 千葉大学総合メディア基盤センター

あらまし　オプティカルフローを用いた移動ロボットのための環境地図生成法と自己運動推定法を提案する。環境地図はロボットが移動可能な領域と障害物領域を固定した座標系で表したものであり、それを生成することは、ロボットの自律行動のために重要な仕事である。本論文では、移動可能領域はロボットから見た視野の半分以上を占めるという仮定を用い、その領域のオプティカルフローを画像列から推定する。そして、推定されたフローから自己運動を推定し、逆投影により環境地図を作成する。実際の移動ロボットにより撮影された画像列を用い、自己運動推定と環境地図生成の実験結果を示す。

Environmental map generation and ego-motion estimation from optical flow for robot navigation

Naoya OHNISHI†　and　Atsushi IMIYA††

†School of Science and Technology, Chiba University
††IMIT

Abstract　In this paper, we aim to develop an algorithm for the construction of an environmental map using optical flow observed through a vision system mounted on an autonomous mobile robot. Our algorithm first detects an area corresponding to the planar area from a sequence of images by employing optical flow, and second, backprojects the planar area to the environment for the construction of an environmental map. Moreover, our algorithm estimates ego-motion of the mobile robot using projected optical flow. The planar area detection by our method does not require any physical assumptions concerning the robot motion or any camera calibration. Therefore, our algorithm allows obstacles to be detected without using any models in the database or any heuristics rule. We show the results of the construction of an environmental map using the mobile robot.

1　Introduction

In this paper, we aim to develop an algorithm for the construction of environmental maps using optical flow observed through a vision system mounted on an autonomous mobile robot. The mobile robot moves over a planar area (e.g., floors and ground) and must avoid collision with obstacles. Therefore, environmental map construction is an essential task for the autonomous navigation and path planning for mobile robots. We assume that the environmental map describes the planar area and other areas from a top view of a fixed coordinate system. Therefore, the environmental map enables the robot to move about the planar area without collision with obstacles.

For the construction of an environmental map, we must detect the planar area in the image sequence observed by the mobile robot. There are many methods for the detection of planar areas in vision systems [1]. For example, edge detection of omni-, and monocular camera systems [2] and the observation of landmarks [3] are classical ones. Since these methods are dependent on the environment around a robot, they involve difficulties, such as the need to predetermine landmarks, when applied to general environments. If a robot captures an image sequence of moving objects, the optical flow[4] [5][6], which is the flow of movement in the scene, is obtained for the fundamental features to generate environment information around the mobile robot. Additionally, optical flow is considered to be fundamental information for obstacle detection in the context of biological data processing [7]. Therefore, the use of optical flow is an appropriate method for the construction of environmental maps from the viewpoint of the affinity between the robot and human beings.

For planar area detection, we apply the idea of a dominant plane. The dominant plane is the planar area that occupies the largest domain in the image observed by a camera. Therefore, the problem of pla-

nar area detection is described as that of dominant plane detection in an image sequence. We show that the dominant plane in a pair of images is combined with affine transformation when the mobile robot obtains successive images for optical flow computation. Therefore, our algorithm allows the dominant plane to be detected without the need to calibrate the camera or to assume camera displacement, since the computation of optical flow does not require the calibration of camera systems.

Our algorithm first detects an area corresponding to the dominant plane from a sequence of images by employing optical flow, and second, backprojects the dominant plane to the environment for the construction of an environmental map. The dominant plane detection by our method does not require any physical assumptions concerning the robot motion. Furthermore, our algorithm detects the dominant plane without camera calibration. Therefore, our algorithm detects obstacles without using any models in the database or any heuristic rules.

Section 2 presents an algorithm for the detection of the dominant plane using optical flow. Section 3 presents an algorithm for the construction of the environmental map from the sequence of the dominant plane. Experimental results of applying our algorithm are presented in Section 4. We show the results of the estimation of an ego-motion of the mobile robot and the construction of an environmental map using the mobile robot.

2 Dominant plane detection from image sequence

When the mobile robot moves over the ground plane, we obtain successive images which include a dominant plane area and obstacles. Therefore, the optical flow computed from the successive images describes the motion of the dominant plane and obstacles on the basis of camera displacement. Since the corresponding points in the dominant plane of an image sequence are combined by an affine transformation, we can compute the affine coefficients in Eq.(3) from optical flow on the dominant plane. Once the affine coefficients are computed, we can estimate the dominant plane motion in the image sequence from the affine coefficients. The dominant plane motion is described by a *planar flow field*, as shown in Fig.1. The difference between the estimated planar flow field and the computed optical flow field enables us to detect the dominant plane area on the image by matching the flow vectors on the image planes.

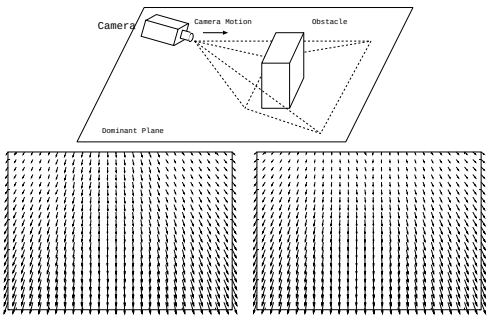

Figure 1: Planar flow of image sequence. top: Example of camera displacement and the environment. left: Computed optical flow. right: Estimated planar flow. In a top-middle area, where exists the obstacle, the length of optical flow is bigger than planar flow.

2.1 Approximation of the dominant plane motion by affine transformation

Setting $\mathbf{H}$ to be the 3×3 matrix [8], the homography between the two images of a planar surface is expressed as

$$\mathbf{p} = \mathbf{H}\mathbf{p}', \tag{1}$$

where $\mathbf{p} = (u, v, 1)^\top$ and $\mathbf{p}' = (u', v', 1)^\top$ are the corresponding points on the two images. The matrix $\mathbf{H}$ is expressed as

$$\mathbf{H} = \mathbf{K}(\mathbf{R} + \mathbf{t}\mathbf{n}^\top)\mathbf{K}^{-1}, \tag{2}$$

where $\mathbf{K}$, $\mathbf{R}$, $\mathbf{t}$, and $\mathbf{n}$ are the projection matrix, the rotation matrix, the translation vector, and the plane normal of the planar surface, respectively. The matrixes $\mathbf{K}$ and $\mathbf{K}^{-1}$ are affine transformations since these matrixes are the projection matrix of a pinhole camera. Assuming that the camera displacement is small, the matrix $\mathbf{R}$ and the matrix $\mathbf{t}\mathbf{n}^\top$ are approximated by an affine transformation. These geometrical and mathematical assumptions are valid when the camera is mounted on a robot moving over the dominant plane. These assumptions allow us to describe the relationship between (u', v') and (u, v) as an affine transformation, such as

$$\begin{pmatrix} u' \\ v' \end{pmatrix} = \begin{pmatrix} a & b \\ d & e \end{pmatrix} \begin{pmatrix} u \\ v \end{pmatrix} + \begin{pmatrix} c \\ f \end{pmatrix}. \tag{3}$$

In the next section, we develop an algorithm for the estimation of these six parameters, a,b,c,d,e, and f, from a sequence of images.

2.2 Planar flow estimation

First, using a pair of successive images from a sequence of images obtained from the camera during robot motion, we compute the optical flow field $(\dot{u}, \dot{v})$. Since

optical flow is the correspondence of dense points between an image pair, Eq.(3) can be applied to each point on the dominant plane. Let (u, v) and (u', v') be the points of the corresponding image coordinates in the two successive images. Point (u', v') can be calculated by adding the flow vector $(\dot{u}, \dot{v})$ to (u, v), if (u, v) and (u', v') are a pair of corresponding points. Thus, by setting $(\dot{u}, \dot{v})$ to be the optical flow at point (u, v) in the image coordinate system, we have the relation

$$\begin{pmatrix} u' \\ v' \end{pmatrix} = \begin{pmatrix} u \\ v \end{pmatrix} + \begin{pmatrix} \dot{u} \\ \dot{v} \end{pmatrix}. \tag{4}$$

If we obtain (u, v) and (u', v'), we can compute the affine coefficients in Eq.(3). If three points are non-collinear, Eq.(3) has a unique solution. Since the dominant plane occupies the largest domain in the image, we select three points randomly to compute the affine coefficients in the successive pair of images. After we compute the affine coefficients, using Eq.(3) again, we can compute the motion of the image sequence of the dominant plane, that is, the collection of corresponding points

$$\begin{pmatrix} \hat{u} \\ \hat{v} \end{pmatrix} = \begin{pmatrix} u' \\ v' \end{pmatrix} - \begin{pmatrix} u \\ v \end{pmatrix} \tag{5}$$

in the image sequence can be regarded as motion flow of the dominant plane on the basis of camera displacement. We call this flow *planar flow* $(\hat{u}, \hat{v})$.

2.3 Dominant plane detection

Setting ε to be the tolerance of the difference between the optical flow vector and the planar flow vector, if

$$\left| \begin{pmatrix} \dot{u}_t \\ \dot{u}_t \end{pmatrix} - \begin{pmatrix} \hat{u}_t \\ \hat{u}_t \end{pmatrix} \right| < \varepsilon \tag{6}$$

is satisfied, we accept point (u_t, v_t) as a point in the dominant plane.

If at least one point on the obstacle area in the image is selected for the estimation of the planar flow, this planar flow is no longer the dominant plane motion. Therefore, the detected dominant plane area is very small. Since the dominant plane occupies the largest domain in the image, in such cases, it becomes evident that the selection of points is incorrect. In those cases, we consequently select another three points randomly. Figure 2 shows examples of each case.

Once we have detected the dominant plane in a certain frame of the image sequence, the planar flow of subsequent images can be estimated robustly using the least-squares method, because dense optical flows are used for the estimation of affine coefficients. Assuming that the robot displacement is small, the dominant plane in the successive images changes negligibly. Therefore, using optical flow on the estimated

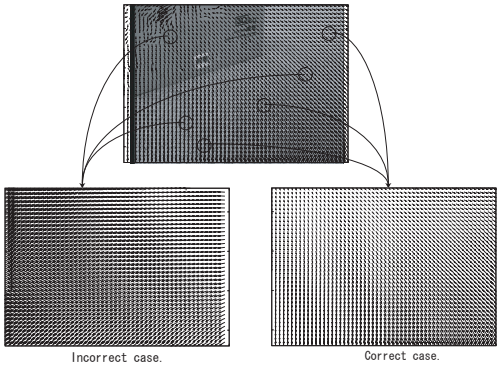

Figure 2: Examples of random sampling. Bottom-left is incorrect case, since the point is selected on the obstacle area. Select another points randomly. Bottom-right is correct case. This planar flow is equal to optical flow in 50% or more of area.

dominant plane in the previous image, we estimate the affine coefficients using the least-squares method. Setting (u_i, v_i) and (u'_i, v'_i) $(0 \leq i \leq n)$ to be corresponding points, the mean-squared errors E_u and E_v associated with Eq.(3) are

$$E_u = \sum_{i=1}^{n} \{u'_i - (au_i + bv_i + c)\}^2, \tag{7}$$

$$E_v = \sum_{i=1}^{n} \{v'_i - (du_i + ev_i + f)\}^2, \tag{8}$$

where n is the number of points used for estimation. Therefore, we can compute affine coefficients which minimize errors E_u and E_v.

2.4 Procedure for dominant plane detection

Our algorithm is summarized as follows.

1. Compute optical flow $(\dot{u}, \dot{v})$ from two successive images.
2. Compute affine coefficients in Eq.(3) by random selection of three points.
3. Estimate planar flow $(\hat{u}, \hat{v})$ from affine coefficients.
4. Match the computed optical flow $(\dot{u}, \dot{v})$ and estimated planar flow $(\hat{u}, \hat{v})$ using Eq.(6).
5. Detect the dominant plane. If the dominant plane occupies less than half of the image area, then return to step(2).

Figure 3 shows the procedure of dominant plane detection from the image sequence.

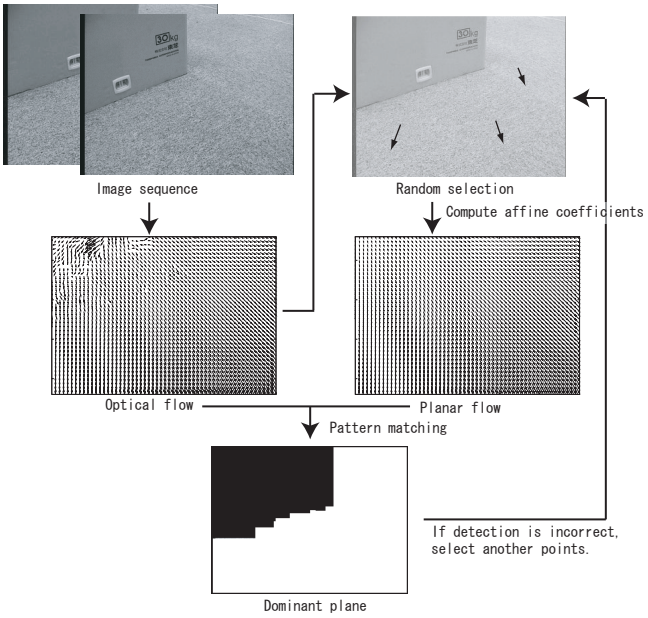

Figure 3: Algorithm for dominant plane detection described in Section 2.3.

3 Environmental map construction

In this section, we develop an algorithm for the construction of the environmental map using planar flow and detected dominant plane.

3.1 Ego-motion estimation from planar flow

We first fix the origin of the world coordinate system at an appropriate point in the environment within which our robot moves. Furthermore, we assume that the origin of the robot coordinate system is initially located at the origin of the world coordinate system. The robot coordinate system moves relative to robot motion. Since the origin of the robot coordinate system moves, to generate an environmental map, we need to know the trajectory of the origin of the robot coordinate system. Using the ego-motion of the robot and the geometrical configuration of the camera system on the robot, we can find the location of the origin of the robot coordinate system. The origin of the camera coordinate system is located at the origin of the robot coordinate system at height H, and the angle between the optical axis of the camera and the vertical axis is angle θ. The relationships between these coordinate systems are shown in Fig.4. Setting (X, Y, Z), (X_R, Y_R, Z_R), and (X_C, Y_C, Z_C) to be the world coordinate system, the robot coordinate system and the camera coordinate system, respectively, the relationship among these coordinate systems is described as

$$\begin{pmatrix} X_R \\ Y_R \\ Z_R \end{pmatrix} = \begin{pmatrix} -1 & 0 & 0 \\ 0 & \cos\theta & \sin\theta \\ 0 & \sin\theta & -\cos\theta \end{pmatrix} \begin{pmatrix} X_C \\ Y_C \\ Z_C \end{pmatrix} + \begin{pmatrix} 0 \\ 0 \\ H \end{pmatrix}. \quad (9)$$

Since we assume that the dominant plane in an image is a collection of points on the plane with $Z = 0$, a point on the dominant plane corresponds to coordinates $(X, Y, 0)$. Therefore, if the camera motion is estimated between time t and time $t+1$, we can detect the ego-motion of the mobile robot and the location of the robot in the fixed coordinate system.

The planar flow on the image plane describes the motion of the dominant plane between time t and time $t + 1$ relative to camera displacement. As shown in Fig.5, the projections of planar flow to the dominant plane yield the flow vector of each point on the dominant plane. The flow vectors on the dominant plane describe the camera motion relative to the dominant plane.

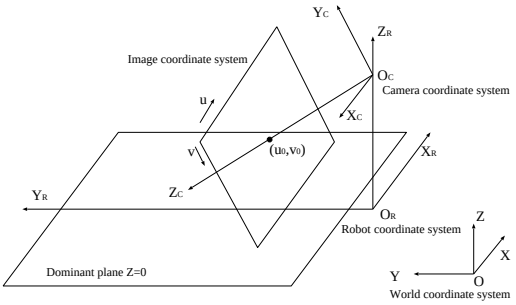

Figure 4: Coordinates of the camera and the dominant plane. (u, v): Image coordinate system. (X_C, Y_C, Z_C): Camera coordinate system. (X_R, Y_R, Z_R): Robot coordinate system. (X, Y, Z): World coordinate system. The dominant plane is the plane with $Z = 0$.

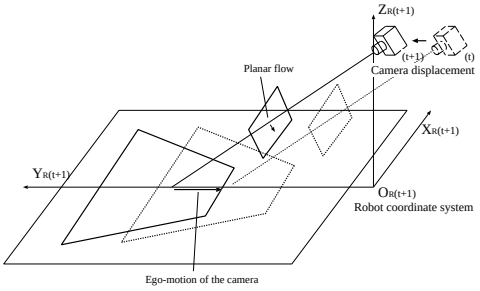

Figure 5: Projected planar flow vector describing ego-motion of the camera relative to the dominant plane.

In Fig.6, the point (u, v) in the image coordinate system is projected onto the point $(X_R(u, v), Y_R(u, v))$ on the dominant plane in the robot coordinate system

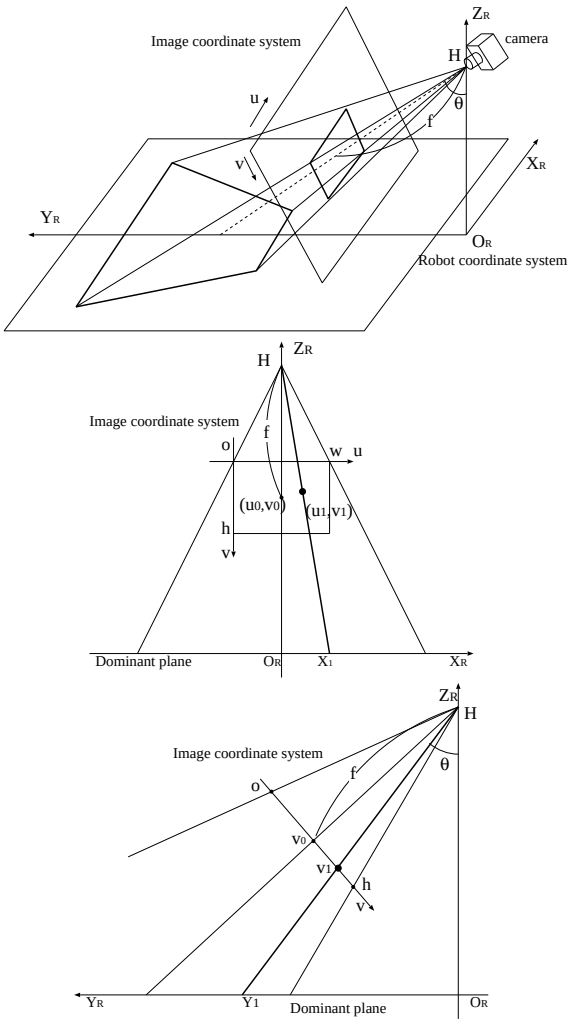

Figure 6: Coordinates of the camera and the dominant plane. (u, v): Image coordinate system. (X_r, Y_r, Z_r): Robot coordinate system. f: Focal length of the camera. H: Distance from the dominant plane to the camera centre. θ: Tilt angle of the camera system from the vertical direction towards the Y axis.

as follows:

$$X_R(u,v) = \frac{H(u-u_0)}{f\cos\theta + (v-v_0)\sin\theta}, \quad (10)$$

$$Y_R(v) = \frac{H(f\sin\theta + (v_0-v)\cos\theta)}{f\cos\theta + (v-v_0)\sin\theta}, \quad (11)$$

where (u_0, v_0) and f are the coordinates of the optical centre of the camera in the camera coordinate system and the focal length, respectively. Therefore, setting $(\hat{X}, \hat{Y})$ to be the planar flow projected onto the dominant plane, projected planar flow $(\hat{X}, \hat{Y})$ and planar flow $(\hat{u}, \hat{v})$ are related by

$$\hat{X} = X(u+\hat{u}, v+\hat{v}) - X(u,v), \quad (12)$$

$$\hat{Y} = Y(v+\hat{v}) - Y(v). \quad (13)$$

Examples for the projection are show in Figs.7 and 8. The projected planar flow $(\hat{X}, \hat{Y})$ describes the

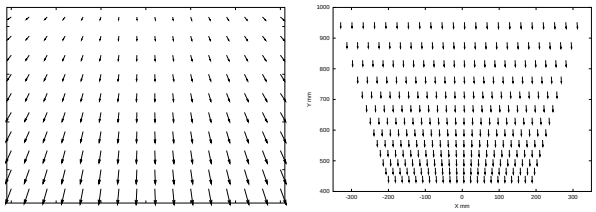

Figure 7: Example of planar flow relative to the forward motion of the mobile robot. left: Planar flow on the image plane. right: Planar flow projected onto the dominant plane.

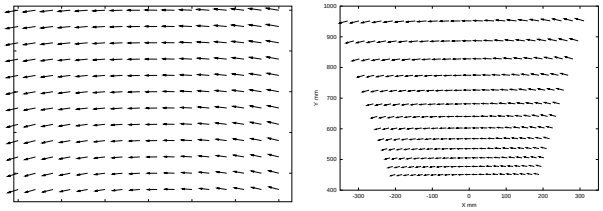

Figure 8: Example of planar flow relative to the rotational motion of the mobile robot. left: Planar flow on the image plane. right: Planar flow projected onto the dominant plane.

displacement of the dominant plane. This displacement combines the translation and the rotation of the dominant plane relative to the camera motion.

Setting $(T_X(t), T_Y(t))$ and $\Omega_Z(t)$ to be the translation vector and the rotation angle at time t, the relationship between point $(X_R(t), Y_R(t))$ on the dominant plane and the corresponding point $(X_R(t+1), Y_R(t+1))$ at time $(t+1)$ is described as

$$\begin{pmatrix} X_R(t+1) \\ Y_R(t+1) \end{pmatrix} = \begin{pmatrix} \cos\Omega_Z(t) & -\sin\Omega_Z(t) \\ \sin\Omega_Z(t) & \cos\Omega_Z(t) \end{pmatrix} \begin{pmatrix} X_R(t) \\ Y_R(t) \end{pmatrix} + \begin{pmatrix} T_X(t) \\ T_Y(t) \end{pmatrix}. \quad (14)$$

Since the algorithm in Section 2.2 yields planar optical flow, Eqs.(10) and (11) define the pair of points $(X_R(t+1), Y_R(t+1))$ and $(X_R(t), Y_R(t))$. Using Eq.(14) allows us to estimate the translation $(T_X(t), T_Y(t))$ and the rotation $\Omega_Z(t)$ by the least-squares method.

The estimation of the robot ego-motion parameters $(T_X(t), T_Y(t))$ and $\Omega_Z(t)$ at time t yields the location of the robot in the world coordinate system at time t. To determine the location of the mobile robot in the dominant plane, we apply SE(2)[9], the special Euclidean group of rigid-body motion in two dimensions.

$$SE(2) = \left\{ \begin{pmatrix} \mathbf{R} & \mathbf{t} \\ 0 & 1 \end{pmatrix} | \mathbf{R} \in \mathbb{R}^{2\times 2}, \mathbf{t} \in \mathbb{R}^2, \right.$$

$$\mathbf{R}^\top \mathbf{R} = \mathbf{I}, \det(\mathbf{R}) = 1 \Big\}, \quad (15)$$

using SE(2), we have the relationship

$$\begin{pmatrix} X_R(t+1) \\ Y_R(t+1) \end{pmatrix} = \mathbf{R} \begin{pmatrix} X_R(t) \\ Y_R(t) \end{pmatrix} + \mathbf{t}. \quad (16)$$

For the estimation of the trajectory of the coordinate system, setting $(P_X(t), P_Y(t))$ and $(P_X(t+1), P_Y(t+1))$ to be the locations of the robot at times t and $t+1$ in the world coordinate system, the location $(P_X(t+1), P_Y(t+1))$ is expressed as

$$\begin{pmatrix} P_X(t+1) \\ P_Y(t+1) \end{pmatrix} = \begin{pmatrix} P_X(t) \\ P_Y(t) \end{pmatrix} + \begin{pmatrix} \cos\Omega_Z & \sin\Omega_Z \\ -\sin\Omega_Z & \cos\Omega_Z \end{pmatrix} \begin{pmatrix} T_X(t) \\ T_Y(t) \end{pmatrix} \quad (17)$$

where $\Omega_Z = \sum_{i=0}^{t} \Omega_Z(i)$. Equations (17) are illustrated in Fig.9 and Fig.5.

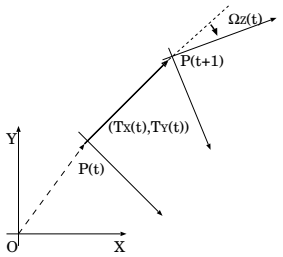

Figure 9: Ego-motion $(T_X(t), T_Y(t))$ and $\Omega_Z(t)$ of the mobile robot. The robot moves from point $P(t)$ to point $P(t+1)$ at time t in the world coordinate system.

3.2 Map construction by backprojection

We construct the two-dimensional environmental map from planar and nonplanar areas of the image sequence by backprojection[10].

In Fig.6, point (u, v) in the image coordinate system is projected to point $(X_R, Y_R, 0)$ on the dominant plane in the robot coordinate system, using Eqs.(10) and (11). Since we estimate the location of the mobile robot in the world coordinate system from Eq.(17), the dominant plane in the robot coordinate system is transformed to the dominant plane in the world coordinate system using the relation

$$\begin{pmatrix} X \\ Y \end{pmatrix} = \begin{pmatrix} \cos\Omega_Z(t) & -\sin\Omega_Z(t) \\ \sin\Omega_Z(t) & \cos\Omega_Z(t) \end{pmatrix} \begin{pmatrix} X_R \\ Y_R \end{pmatrix} + \begin{pmatrix} P_X(t) \\ P_Y(t) \end{pmatrix}. \quad (18)$$

The dominant plane in the world coordinate system is the area in which the robot can move. Therefore, we can construct an environmental map relative to the displacement of the mobile robot.

Table 1: The location (X, Y) in the world coordinate system in last frame. T0 ... T5 are results of the estimation with initial frames 0 ... 5 of the image sequence, respectively.

	T0	T1	T2	T3	T4	T5
P_X	-10.7	-9.9	-10.0	-10.6	-10.5	-9.6
P_Y	681.6	678.2	679.1	677.9	680.5	679.8

4 Experiment

In this section, we show some results of ego-motion estimation and environmental map generation using a real image sequence observed through the camera mounted on a mobile robot.

4.1 Ego-motion estimation

We show the results of experiments for ego-motion estimation of the mobile robot using a real image sequence. The robot moves forward toward the obstacle, as shown in Fig.10. For the evaluation of the robustness and the accuracy of our algorithm, we estimate the ego-motion of the robot using images observed during one robot motion. and change the initial location and the step interval of the image sequence. The robot is located at the origin of the world coordinate system in frame 0, and moves forward along the direction of the Y axis.

First, we estimate the robot motion using frame t and frame $t+6$ of the image sequence and change the initial location t from $t = 0$ to $t = 5$. We set T0 to be the result of estimation with $t = 0$, that is, using $(0, 6, 12, \ldots)$ frames of the image sequence. In the same manner, we set T1, T2, T3, T4 and T5 to be the results of the estimations with $t = 1, 2, 3, 4$ and 5, respectively. The result of the estimations is shown in figure 11, and Fig.11(b) shows an enlargement of figure 11(a). In figures 11(a) and 11(b), X and Y axes are those of the world coordinate system, and lines and dots are the estimated paths and locations of the mobile robot $(P_X(t), P_Y(t))$ in Eq.(17), respectively. Table 1 shows the location of the mobile robot in the last frame.

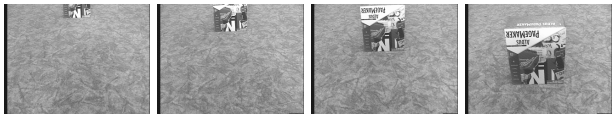

Figure 10: Image sequence of translational motion. From the left, the image at frames 100, 200, 300 and 400.

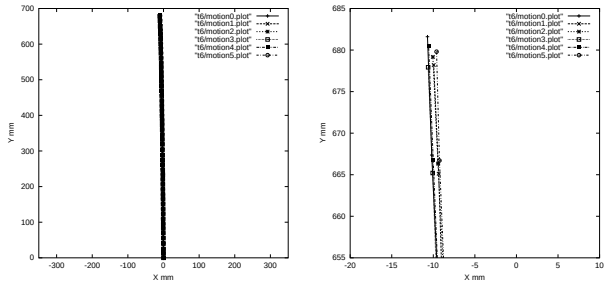

(a) (b)

Figure 11: (a) Result of the estimation of translational motion for different initial frames. Lines and dots are estimated paths and locations of the mobile robot, respectively. (b) Enlargement of (a).

The results in Fig.11(a) and Tab.1 indicate that the difference in the location in the last frame is about 0.9 % relative to the distance moved by the robot, about 680mm. Therefore, we can conclude that our algorithm of ego-motion estimation is robust for various initial locations of the robot.

Next, we estimate the robot motion starting at frame $t = 0$ using the image sequence frame t and frame $t + s$, where the step interval s is $4, \ldots, 8$. We set S0 to be the result of estimation with $s = 4$, that is, using $(0, 4, 8, \ldots)$ frames of the image sequence. In the same way, we set S5, S6, S7 and S8 to be the results of the estimations with $s = 5, 6, 7$ and 8, respectively. The results of the estimations are shown in Fig.12(a), and Fig.12(b) shows an enlargement of Fig. 12. Table 2 shows the location of the mobile robot in the last frame.

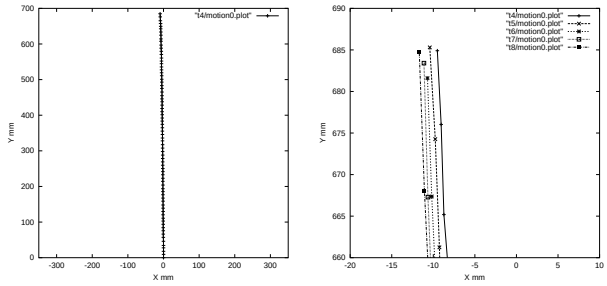

(a) (b)

Figure 12: (a) Result of the estimation of translational motion for a various span of the image sequence. (b) Enlargement of (a).

The results in Fig.12(b) and Tab.2 show that the difference in the location of the robot in the last frame is about 0.7 % relative to the distance moved by the robot. Therefore, our algorithm is robust for different

Table 2: The location (X, Y) in the world coordinate system in last frame. S4 ... S8 are results of the estimation with spans 4 ... 8 of the image sequence, respectively.

	S4	S5	S6	S7	S8
P_X mm	-9.5	-10.4	-10.7	-11.1	-11.6
P_Y mm	684.9	685.3	681.6	683.	684.7

velocities of the mobile robot.

We also estimate the ego-motion of the robot using the image sequence of rotational motion, as shown in Fig.10. The robot is initially located at the origin of the world coordinate system in frame 0, and then rotates about 80 degrees to the right. Figure 14 shows

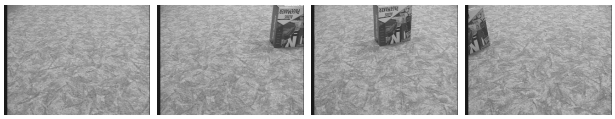

Figure 13: Image sequence of rotational motion. From the left, images at frames 10, 30, 50 and 80.

the result of the estimation of rotational motion.

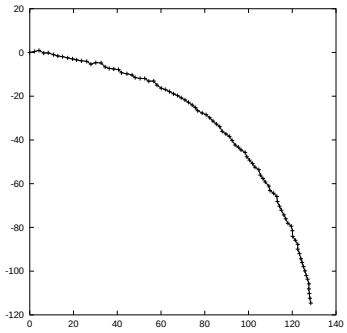

Figure 14: Result of the estimation of the rotational motion.

4.2 Environmental map construction

We experimentally construct the environmental map using Eq.18. Figure 15 show the result of the construction of the environmental map using the image sequence in Fig.10. In Fig.15, X and Y coincide with X and Y axes of the world coordinate system. Furthermore, gray, black and white areas are the estimated planar area, obstacles and areas out of sight. The line represents the path of the mobile robot estimated using Eq.(17).

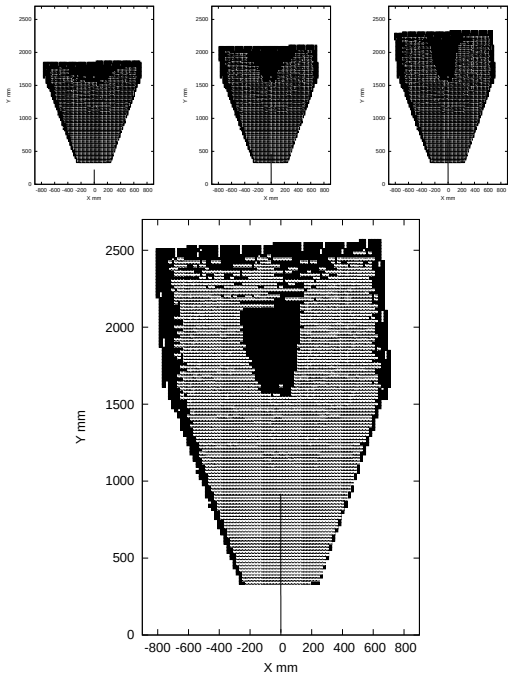

Figure 15: Environmental map at frames 100, 200, 300 and 400. X and Y axes coincide with world coordinate X and Y axes, respectively. Gray, black and white areas are the estimated planar area, obstacles and area out of sight. The line represents the estimated path of the mobile robot.

5 Conclusion

We developed an algorithm for the construction of an environmental map for mobile robot navigation. The algorithm allows the locations of obstacles and the robot to be detected using optical flow computed from the image sequence observed through the camera mounted on the mobile robot. Furthermore, we showed that corresponding points on dominant planes in a pair of successive images are combined by affine transformation. Using this idea, if we compute the affine coefficients which relate the corresponding points in two successive images, we can easily obtain a dense planar flow which expresses a camera motion. This property of the points in a dominant plane allows us to design an algorithm which enables the dominant plane to be detected by simple pattern matching of the flow vectors in a series of dominant planes. Furthermore, planar flow enables us to estimate the path of camera displacement.

Although a model-based approach to dominant plane detection has been proposed in [13], our method is a non-model-based approach. In addition, our algorithm allows the dominant plane to be detected without camera calibration, since our algorithm uses optical flow which does not require the calibration of camera systems and the affine approximation for the correspondence between the same points in a pair of images. Results of experiments using real and artificial image sequences confirmed that the dominant plane can be detected accurately. These experiments allow the application of our method to the navigation and path planning of a mobile robot with a vision system.

References

[1] Guilherme, N. D. and Avinash, C. K., Vision for mobile robot navigation: A survey, IEEE Trans. on PAMI **24**, 237-267, (2002).

[2] Kang, S. B. and Szeliski, R., 3D environment modeling from multiple cylindrical panoramic images, *Panoramic Vision: Sensors, Theory, Applications*, 329-358, Ryad Benosman and Sing Bing Kang, ed., Springer-Verlag, (2001).

[3] Fraundorfer, F., A map for mobile robots consisting of a 3D model with augmented salient image features, 26th Workshop of the Austrian Association for Pattern Recognition, 249-256, (2002).

[4] Barron, J.L., Fleet, D.J., and Beauchemin, S.S., Performance of optical flow techniques, International Journal of Computer Vision, **12**, 43-77, (1994).

[5] Horn, B. K. P. and Schunck, B.G., Determining optical flow, Artificial Intelligence, **17**, 185-203, (1981).

[6] Lucas, B. and Kanade, T., An iterative image registration technique with an application to stereo vision, Proc. of 7th IJCAI, 674-679, (1981).

[7] Mallot, H. A., Bulthoff, H. H., Little, J. J., and Bohrer, S., Inverse perspective mapping simplifies optical flow computation and obstacle detection, Biological Cybernetics, **64**, 177-185, (1991).

[8] Hartley, A. and Zisserman, A., *Multiple View Geometry in Computer Vision*, Cambridge University Press, (2000).

[9] Kanatani, K., *Group-Theoretical Methods in Image Understanding*, Springer-Verlag, (1990).

[10] Laurentini, A., The visual hull concept for silhouette-based image understanding, PAMI, **16**, 150-162, (1994).

[11] Bouguet J.-Y., Pyramidal implementation of the Lucas Kanade feature tracker description of the algorithm, Intel Corporation, Microprocessor Research Labs, OpenCV Documents, (1999).

[12] Rotating Blocks: Otago Optical Flow Evaluation Sequences
website: http://www.cs.otago.ac.nz/research/vision/Research/

[13] Enkelmann, W., Obstacle detection by evaluation of optical flow fields from image sequences, Image and Vision Computing, **9**, 160-168, (1991).